Proceedings of the Ninth Pacific Conference on Earthquake Engineering
Building an Earthquake-Resilient Society
14-16 April, 2011, Auckland, New Zealand

Building seismic ceiling fragility using spectral acceleration

J. Singh

Rose School, Pavia, Italy.

G. A. MacRae, R. P. Dhakal, S. Pampanin

University of Canterbury, Christchurch, New Zealand.

ABSTRACT: Seismic damage to ceilings can cause significant downtime and economic loss in addition to life safety risk. In order to understand this risk and develop mitigation strategies a small project on non-structural damage was recently funded by the FRST Natural Hazards Platform at the University of Canterbury. This project looks at the demands imposed on ceilings in a seismic event. The engineering demand parameter of interest is the total peak floor acceleration. Two different ceiling types are investigated; the "perimeter fixed" and the "floating type" ceiling. Firstly each ceiling type is modelled explicitly with its own mass in a single storey one bay frame to evaluate the changes in response relative to the ceiling above for a number of parameters. Secondly, median peak total floor accelerations for the 10 storey Redbook building are obtained by conducting time history analysis with a suite of 20 ground motion records. Thirdly, this information is combined with ceiling system fragility information based on floor acceleration to obtain the system fragility information based on ground motion parameters.

1 INTRODUCTION

Damage to non-structural components in buildings can result in a loss of functionality and in economic losses even if the structural components are largely damage free. Non-structural elements and building contents make up around 50%-70% of the total building cost in most buildings according to Taghavi and Miranda (2003) as shown in Figure 1. Hence investigating earthquake effects on building non-structural elements is important. The 2010 Canterbury/Darfield earthquake has also shown that non-structural components and contents falling from height may threaten life safety (Dhakal 2010).

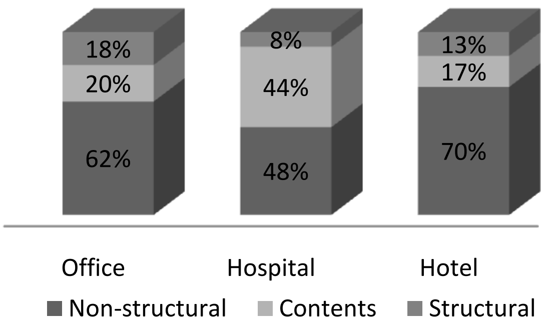

Figure 1: Building Type-Cost Breakdown *(after Taghavi and Miranda 2003)*

2 COMMON TYPES OF CEILINGS

Two common ceiling types are shown in Figure 2. The first ceiling type shown is the *floating ceiling*, which is not connected to the perimeter wall/frame but a stiff connection exists between the ceiling and the floor above to carry the lateral force from the frame. The gap at the ends of the ceiling has to be large enough to accommodate the storey drift demands plus some extra clearance due to additional ceiling response due to flexibility of braces. If the gap on the ends is not sufficient, pounding may take place which could impose very large acceleration demands on the ceiling.

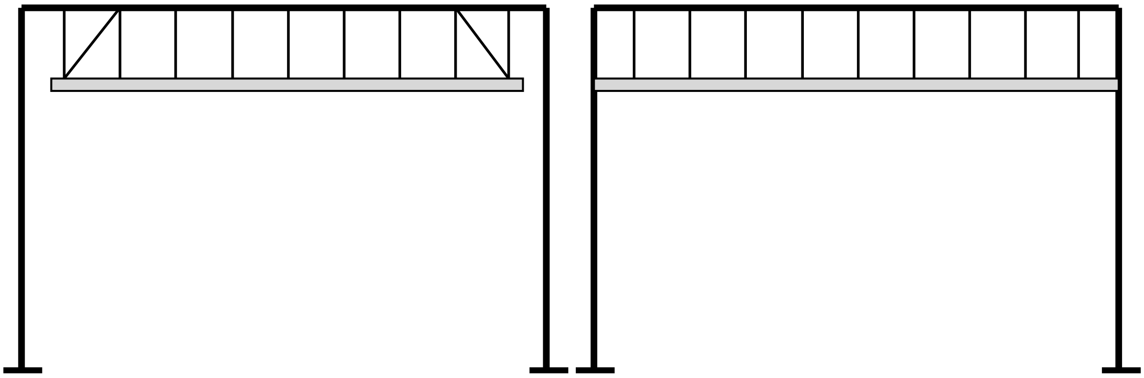

(a) Floating

(b) Perimeter fixed

Figure 2: Floating and Perimeter fixed ceiling types (Grange 2009)

The second ceiling type is the *perimeter fixed ceiling* as shown in Figure 2b. The accelerations in the ceiling are imposed by the columns/walls around the ceiling perimeter. The hangars are simply expected to carry vertical forces. Services connected to the ceiling may induce additional forces in the ceiling members. These services may include lighting fixtures, HVAC fixtures, and fire sprinklers. In particular, sprinklers which are rigidly attached to the ceiling without any gap can induce substantial forces in the ceiling members (Paganotti et al, 2011).

3 CEILING VERSUS FLOOR BEHAVIOUR

For simplicity in analysis, it is easy to assume that ceiling acceleration demands are identical to the acceleration demands of the floor above it. However, because the ceiling may have its own stiffness and mass, the response may be different. This difference in response is quantified below on a one bay single storey frame. The ceiling was assumed to be 6 m x 6 m in plan. Both *perimeter fixed* and *floating* ceiling types were investigated. The analyses were conducted for a range of frame fundamental period and design ductility. The elastic strength of the structure was obtained by trial; the strength of the plastic hinge elements provided at the member ends was varied till there was no energy dissipation in the plastic hinge regions. The member strength at various ductilities was obtained by a simple force reduction factor based on the equal displacement principle. Ceiling weights were $0.05kN/m^2$ and $0.16kN/m^2$ for the light and heavy ceiling respectively. These values were obtained from ceiling companies during discussions. The ceiling mass to floor mass ratio was about 0.9% and 3.0% for the light and heavy ceiling respectively. All members including the structural framing and ceiling were modelled with frame elements. The ceiling hangers were modelled using springs which could only take tension. The Takeda hysteresis rule was used for the frame elements in the plastic hinge regions. The ceiling and floor were assumed to be rigid in all modelling conducted. For the *floating ceiling*, contact elements were used to take into account any pounding that may occur between the structure and ceiling.

(a) Effect on Fundamental Period

Table 1 shows the periods obtained from the inelastic dynamic time history analysis programme RUAUMOKO (Carr, 2010) for the different ceiling types. These results are compared with the results obtained if the masses and ceiling are lumped which would be the easiest analysis option. It may be seen that there is almost no difference in the fundamental mode period for all cases.

Table 1: Comparison of Frame Fundamental Periods

Case	Ceiling and Floor Mass Lumped	Perimeter Fixed Ceiling	Floating Ceiling
1	0.43 s	0.43 s	0.43 s
2	1.15 s	1.14 s	1.15 s
3	2.07 s	2.07 s	2.07 s
4	3.19 s	3.19 s	3.19 s
5	4.49 s	4.49 s	4.49 s

(b) Effect on Ceiling Accelerations

It is observed in Figure 3 that as the inelasticity of the structure increases, the ceiling acceleration becomes marginally higher than the floor acceleration. Generally, the ceiling and floor accelerations for the perimeter fixed ceiling are very similar. The responses of the light and heavy ceiling are also very similar.

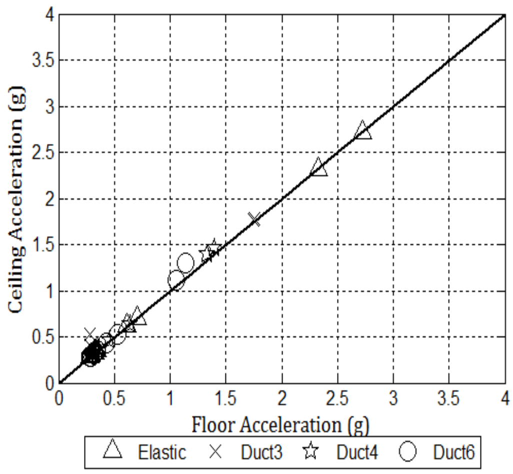

(a) Lighter ceiling (0.05kN/m^2)

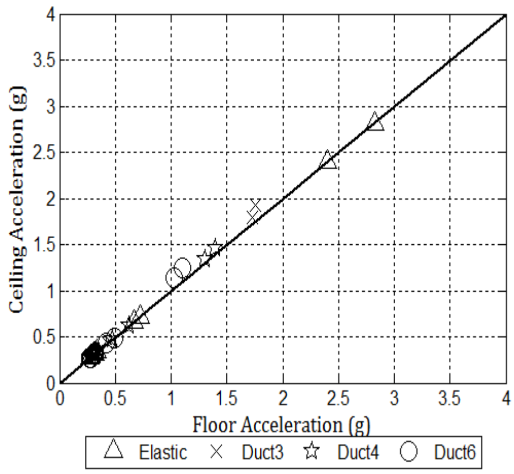

(b) Heavier ceiling (0.16kN/m^2)

Figure 3: Perimeter Fixed Ceiling Accelerations vs. Floor Accelerations

For the *floating ceiling*, an infinitely stiff brace would mean that the floor and ceiling accelerations are identical. For this study it was assumed that there was one ceiling brace from a 40 mm x 40 mm x 0.55 gage steel angle in the direction concerned for the 6m x 6m ceiling. The braces in the *floating ceiling* was attached in a similar way to what is illustrated in Figure 2(a). The brace was modelled using frame elements which were pin ended and inclined at 45 degrees. The ceiling mass was the same as that for the *perimeter fixed* case. Contact elements were used to model any interaction between the surrounding wall/frame with the ceiling. Figure 4 shows that the floor and ceiling accelerations are similar for a large gap. Ceiling acceleration and ductility seem to follow no particular trend in the inelastic cases. The heavier ceiling tended to have slightly greater accelerations than the lighter ceiling. Here the movement of the floor toward the wall was on average about 10 mm when the floor acceleration was 1.0g.

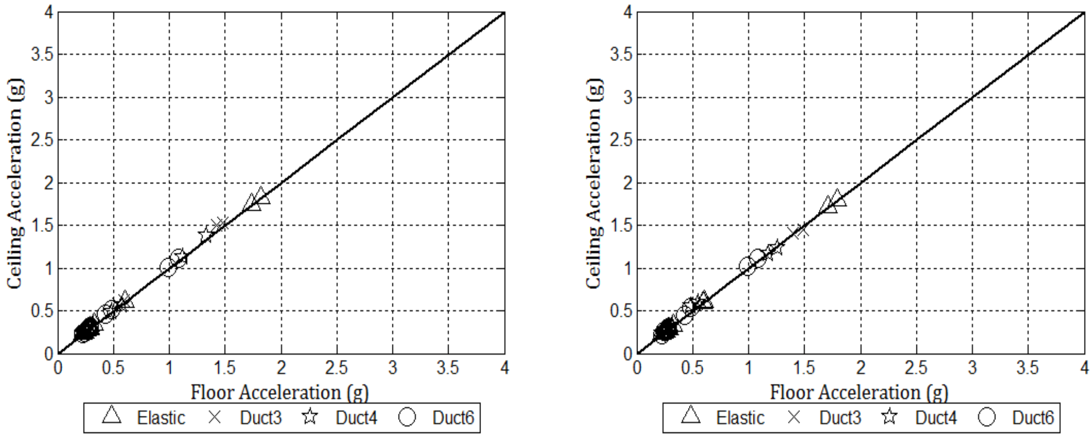

(a) Lighter ceiling ($0.05kN/m^2$)   (b) Heavier ceiling ($0.16kN/m^2$)

Figure 4: Floating Ceiling Acceleration vs. Floor Acceleration for Large Gap

Figure 5 shows the response for the heavier ceiling with gaps between the wall and roof of 8mm and 1mm. In these cases too, the ceiling accelerations were generally larger than the floor accelerations. It may be seen that the ceiling response became nonlinear after the floor accelerations exceeded 1.0g for 8mm perimeter gap. This increased ceiling acceleration is due to pounding between the ceiling and the surrounding wall/frame when the ceiling displacement equalled the gap. Ceilings with lower gaps tend to have greater pounding accelerations which understandably start earlier (i.e. at a smaller displacement). These pounding accelerations show up as a spike in the ceiling acceleration records. These high ceiling accelerations increase the possibility of ceiling damage and failure.

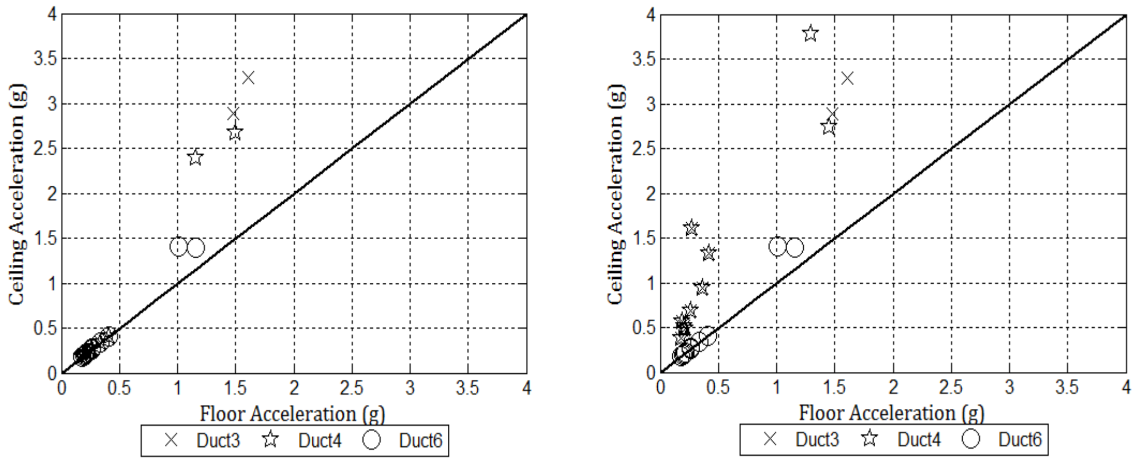

(a) 8 mm Gap   (b) 1 mm Gap

Figure 5: Floating ceiling analysis for Heavier Ceiling ($0.16kN/m^2$)

4 MULTI-STOREY STRUCTURE FLOOR ACCELERATIONS

The NZ “Red-Book” building (Bull, 2008) was used to quantify the floor accelerations for a multi-storey building and to give a quick estimate of the likely losses. This is a concrete frame building, square in plan with a floor area on each level of about 900 m^2. The building is assumed to be located in the central business district of Christchurch. The bottom floor has a storey height of 4 m while the upper floors have a storey height of 3.6 m. Glass fibre reinforced concrete panels are used for the exterior panels. The building is designed to be used as an office and is designed in accordance with NZS1170 (2004) and NZS3101 (2006). The floor plan of the building is shown in Figure 6. The fundamental period of the structure was 2.40 seconds. Rotational springs were used to model the inelastic regions of the frame with the panel zone assumed to be semi-rigid. The stiffness of the panel zones was taken as ten times the beam *EI*, where *E* is the Young's Modulus and *I* is the beam second moment of area.

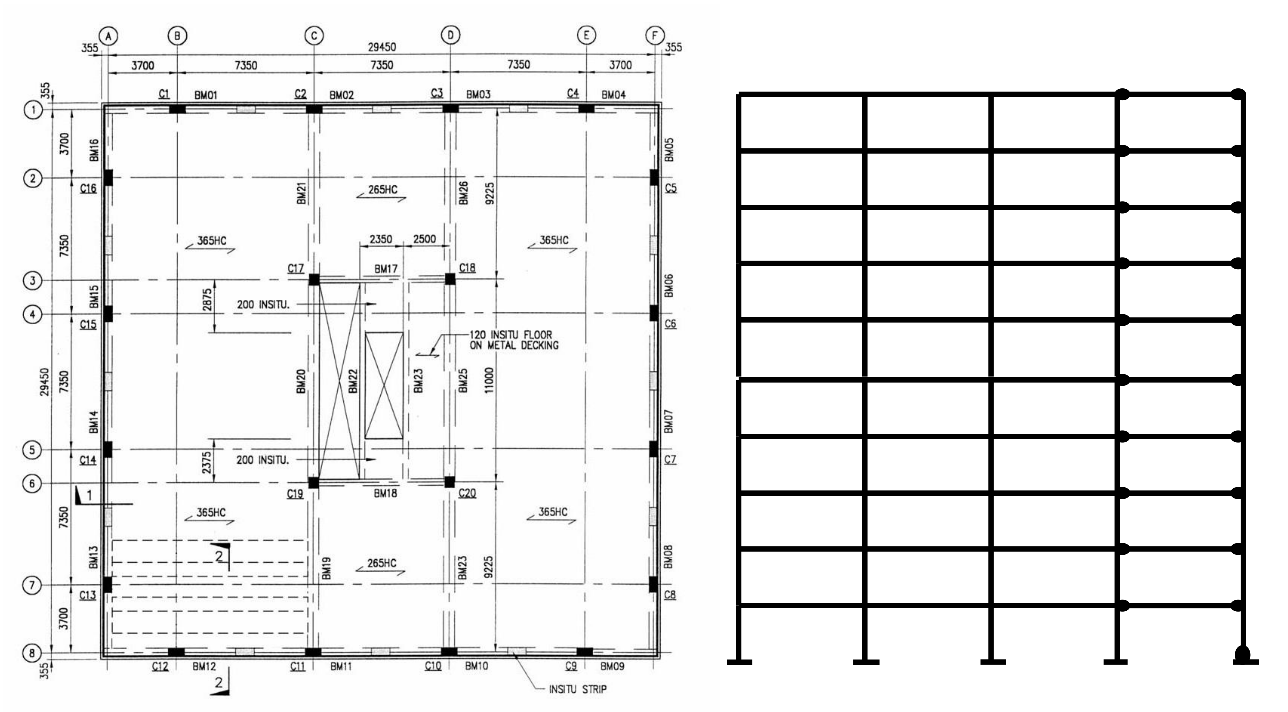

(a) Plan (b) Frame Elevation

Figure 6: Building plan view and frame model with leaning column.

Incremental dynamic analysis (IDA) was conducted. The total floor acceleration was the engineering demand parameter (EDP) and spectral acceleration of each ground motion at the fundamental period of the building as the intensity measure (IM). Twenty SAC ground motion records from the LA 10 in 50 suite (SAC, 1997) were used in the time history analysis in Ruaumoko2D (Carr, 2010). The log-normal median was determined from the peak total floor response accelerations. IDA curves were plotted at every storey. These are shown for the first floor (at the top of the first storey) and for the roof in Figure 7. As the spectral acceleration was increased beyond 0.2g, global collapse was observed for some records. In Figure 7, the markers at total floor acceleration equal to zero indicate that some records resulted in collapse of the building. The median after collapse had occurred in some of the analysis was based on a reduced data set and hence is biased. At a spectral acceleration of 0.3g, six records caused the building to collapse. Similarly, when the spectral acceleration was scaled up further to 0.4g, 0.5g, and 0.6g, more records (8, 11 and 15 respectively) caused the model to collapse.

The EDP-IM relationship in figure 7(a) and 7(b) generally shows that as the spectral acceleration increases, the total floor acceleration also increases. However, as the spectral acceleration gets bigger, the increment in the total floor acceleration was found to decrease. This is opposite to what is normally observed in IDA curves when drift is used as EDP. This behaviour may be attributed to the fact that as the spectral acceleration gets larger the response enters inelastic phase, and the hinges forming at the base of the structure tend to filter the high frequency content of ground motion resulting in a deamplification of total floor accelerations up the height of the structure (Bradley, 2009).

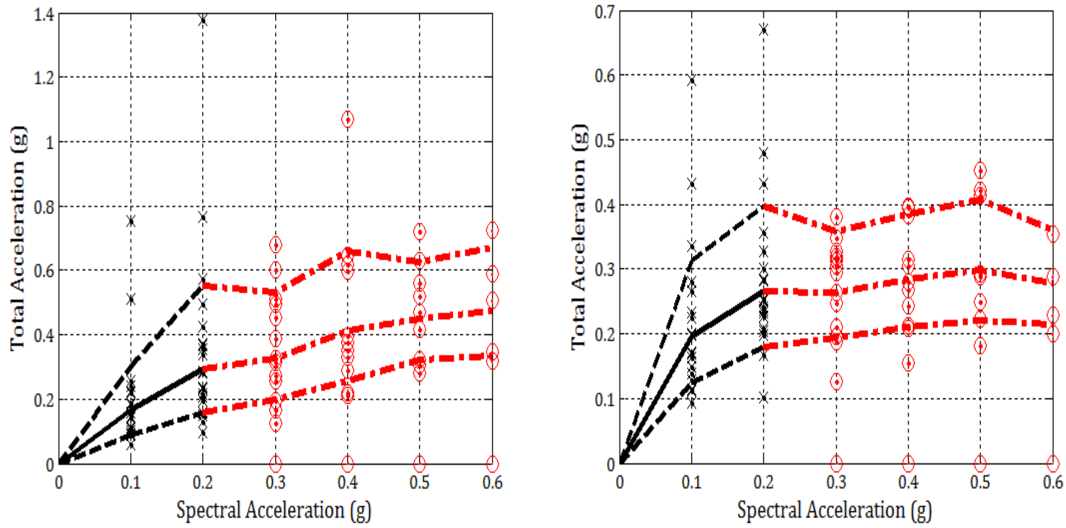

(a) First Floor (b) Roof

Figure 7: IDA curves at different levels

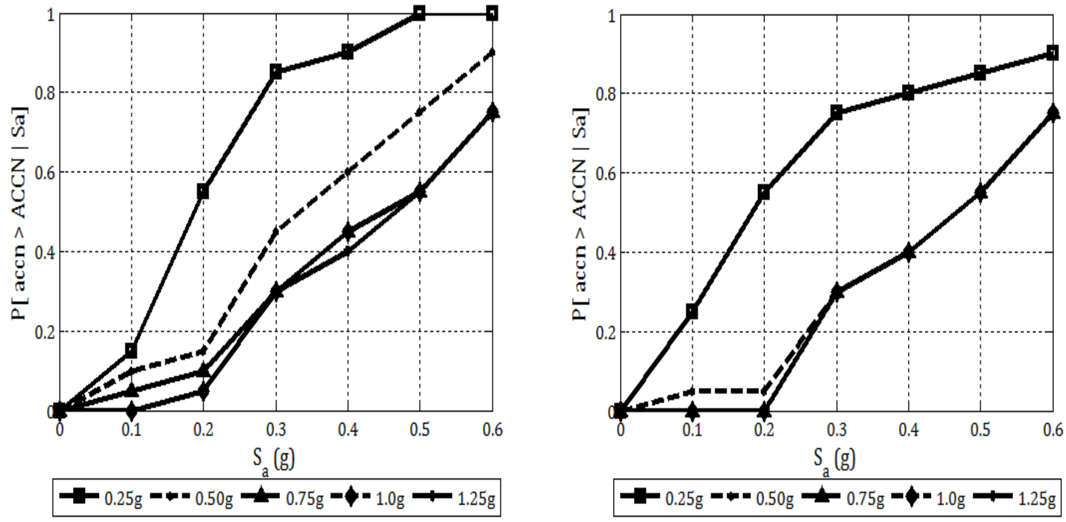

(a) First Floor (b) Roof

Figure 8: Fragility curves

Next, the fragility curves at every level were plotted (as shown in Figure 8 for the ground floor and the roof) based on the total probability theorem (Jalayer, 2003) as shown in Equation 1 where *ACCN* = acceleration corresponding to limit states, $accn_i$ = peak total floor acceleration obtained from analysis, C = collapse and NC = no collapse.

$$P[ACCN > accn_i | Sa_i] = P[ACCN > accn_i | NC, Sa_i] * P[NC | Sa_i] + \ldots\ldots\ldots\ldots P[ACCN > accn_i | C, Sa_i] * P[C | Sa_i] \quad (1)$$

It should be noted that $P[ACCN > accn_i | C, Sa_i]$ was taken as unity. It must be noted that at spectral accelerations lower than 0.2g, the probability of exceedance of a particular limit states is solely due to exceedance for the non-collapse case. On the other hand, for Sa > 0.2g, the probability of a particular limit state being exceeded is a sum of the limit state being exceeded for the non-collapse and collapse cases. Also, the probability of collapse of the model increases as the intensity measure is further scaled up.

Very simple first order estimates of expected economic losses are developed for two different ceiling types. Loss assessments were conducted for a poor ceiling with a median floor acceleration (a_f) of 0.5g and for a low damage ceiling which has a median a_f of 1.0g. The dispersion of both ceiling strengths was assumed to be 0.4. The probability of damage at every floor was approximated at a spectral acceleration of 0.2g from the respective demand fragility curves at every floor level. The ceiling capacity fragility data is based on a ceiling which is 3mx6m in area. The replacement cost of the ceiling is $30/m^2 (obtained from discussions with a particular ceiling company) and the total ceiling area per storey is assumed to be 900m^2; i.e. equal to the total floor area.

Table 2 shows the calculation of the loss incurred in each floor. Note that the values in the second and 4th columns are taken directly from the fragility curves plotted for the two ceiling system. For example; Figures 7a and 8a show that 0.15 (3 out of 20) is the probability that the first floor acceleration will exceed 0.5g; and hence 0.15 is the value adopted in the Table. Similarly, by using the fragility curves of all floors, the corresponding probabilities can be obtained to populate Table 2. The damage cost was then obtained by multiplying the probability of exceedance of the given floor acceleration by the total ceiling area per floor (i.e. 900 m^2) and the installation cost of the ceiling per unit area (i.e. $30/m^2).

Table 2: Probability of Damage and Damage Cost at Each Floor Level for Different Ceiling Types

Floor	Ceiling with median strength 0.5g		Low Damage Ceiling with median strength 1g	
	P[a_f > 0.5g | Sa =0.2 g]	Damage Cost ($)	P[a_f > 1.0g | Sa =0.2 g]	Damage Cost ($)
1	0.15	$4050	0.05	$1350
2	0.15	$4050	0	0
3	0.1	$2700	0	0
4	0.1	$2700	0	0
5	0.1	$2700	0	0
6	0.1	$2700	0.05	$1350
7	0.1	$2700	0	0
8	0.1	$2700	0	0
9	0.05	$1350	0	0
10	0.05	$1350	0	0
	Total Damage Cost	**$27,000**		**$2,700**

The total cost of replacing/repairing the weaker ceiling for this particular scenario of S_a= 0.2g is $27,000, whereas the total cost of replacing/repairing the low damage ceiling is $2700 only, which is ten times less than the damage cost of the weaker ceiling. This indicates that increasing the ceiling performance can result in a significant saving of loss during an earthquake.

5 CONCLUSIONS

Several analyses were conducted to evaluate the performance, likely demands, likely damage and loss of different building types. It was found that:

1) For floating ceilings with sufficient clearance which do not impact with the surrounding frame/wall; the ceiling accelerations could be reasonably approximated by the floor accelerations. When impact occurs significantly greater accelerations are induced. For the perimeter fixed ceilings, the ceiling and floor accelerations are very similar. Heavy ceilings tend to have slightly greater accelerations in all cases.

2) Floor acceleration demands were obtained for a suite of records for the different levels of the 10 storey Red Book building.

3) Using the information from 1 and 2, as well as some assumed fragility curves, the probability of failure at different levels of the Red Book building were obtained for two different ceiling systems.

4) A first order estimate of the cost due to damage was made using the information obtained from 1 to 3, as well as a typical unit cost of ceilings. It was shown that low-damage ceilings, which have higher strength, are likely to suffer significantly less loss than weaker ceilings do in earthquakes.

6 REFERENCES

Bradley, B. A. (2009) Structure Specific Probabilistic Seismic Risk Assessment. *PhD Thesis*, Department of Civil and Natural Resource Engineering, University of Canterbury, Christchurch, New Zealand.

Bull, D. K. and Brook, R. (2008) Examples of Concrete Structural Design to Standards NZS3101. New Zealand

Carr, A. J. (2010) Ruaumoko2N: Dynamic Analysis of 2 Dimensional Inelastic Structures. Department of Civil Engineering, University of Canterbury, Christchurch, New Zealand.

Dhakal R. P. Damage to Non-Structural Components and Contents in 2010 Darfield Earthquake, *Bulletin of the NZ Society of Earthquake Engineering*, 43(4): 404-411, Dec 2010

Grange P. 2009. Assessment and Mitigation of Seismic Ceiling System Damage. *MASTERS OF ENGINEERING RESEARCH PROPOSAL*, University of Canterbury, December.

Jalayer, F. (2003). Direct Probabilistic Seismic Analaysis: Implementing Non-linear Dynamic Assessments. *PhD Thesis*, Department of Civil and Environmental Engineering, Stanford University.

Paganotti G. Dhakal R, and MacRae G. A. Development of Typical NZ Ceiling System Seismic Fragilities, Proceedings of the Ninth Pacific Conference on Earthquake Engineering, 14-16 April, 2011, Auckland, New Zealand

SAC Steel (1997) Project Title: Develop Suites of Time Histories. Project Task 5.4.1. Subcontractors: Woodward-Clyde Federal Services, Pasadena. [Online]. Available: http://nisee.berkeley.edu/data/strong_motion/sacsteel/ground_motions.html [2008, September 2]

Taghavi, S. and Miranda, E. (2003) Response Assessment of non-structural building elements. Report No. 2003/05. Pacific Earthquake Engineering Research Center, Richmond, CA.